II CONGRESSO NACIONAL DE ENGENHARIA MECÂNICA
II NATIONAL CONGRESS OF MECHANICAL ENGINEERING
12 a 16 de Agosto de 2002 - João Pessoa – PB

MODELING THE WELD BEAD GEOMETRY FOR KEYHOLE PLASMA WELDING OF AISI 304L STAINLESS STEEL

André Richetti
Universidade Federal de Uberlândia, Faculdade de Engenharia Mecânica, Uberlândia, MG, Brasil. E-mail: arichett@mecanica.ufu.br

Sonia A. G. Oliveira
Universidade Federal de Uberlândia, Faculdade de Engenharia Mecânica, Uberlândia, MG, Brasil. E-mail: sgoulart@mecanica.ufu.br

Valtair Antonio Ferraresi
Universidade Federal de Uberlândia, Faculdade de Engenharia Mecânica, Uberlândia, MG, Brasil. E-mail: valtairf@mecanica.ufu.br

Abstract. *The new tendencies that came from the worldwide globalization have risen the competition between enterprises, which must adapt to the market changes quickly. In order to do that, high investments are used to optimize the processes, combining productivity, quality and competitiveness to the final product. In this sense, the keyhole plasma arc welding is a good alternative and has received a significant acceptance for automated applications in the last years. Many strategies have been used for the welding applications development, such as the evaluation of models that allow predicting the process behavior under certain conditions. The aim of this work is the development of an empirical model for the AISI 304L stainless steel keyhole weld bead geometry. This model was obtained using a methodology based on the Similitude Theory and as process variables was used the current, the welding speed and plasma gas flow rate. The model was proposed to predict the weld bead geometry, allow the process optimization and give support to the understanding of the involved phenomena. The results proved the model consistency and the prediction of the weld bead geometry with adequate precision and safety.*

Keywords: *Plasma arc welding, Keyhole, Similitude, Empirical modeling, Optimization.*

1. INTRODUCTION

The keyhole plasma welding, illustrated in Fig (1), have had a significant acceptance in the last years for its use in automated applications which involve weld quality, productivity and assurance of total joint penetration. Actually, this process appears as a promising alternative to other conventional welding processes and its technology is already well known in developed countries. Applications of the plasma process are constantly increasing due the need of fabrication quality and productivity improvements provoked by the worldwide market globalization.

However, there are still some difficulties concerning the welding parameter set, which normally is made, based on the welder skill or by equipment manufacturers recommendations. Such conditions, nevertheless, are out of the optimal conditions, affecting both the productivity and quality and adding

extra costs to the final product. This problem occurs also due to the practical difficulty to act directly into the process for its optimization. The process optimization has been got through the evaluation of mathematical models, which allow predicting the process behavior under certain work conditions.

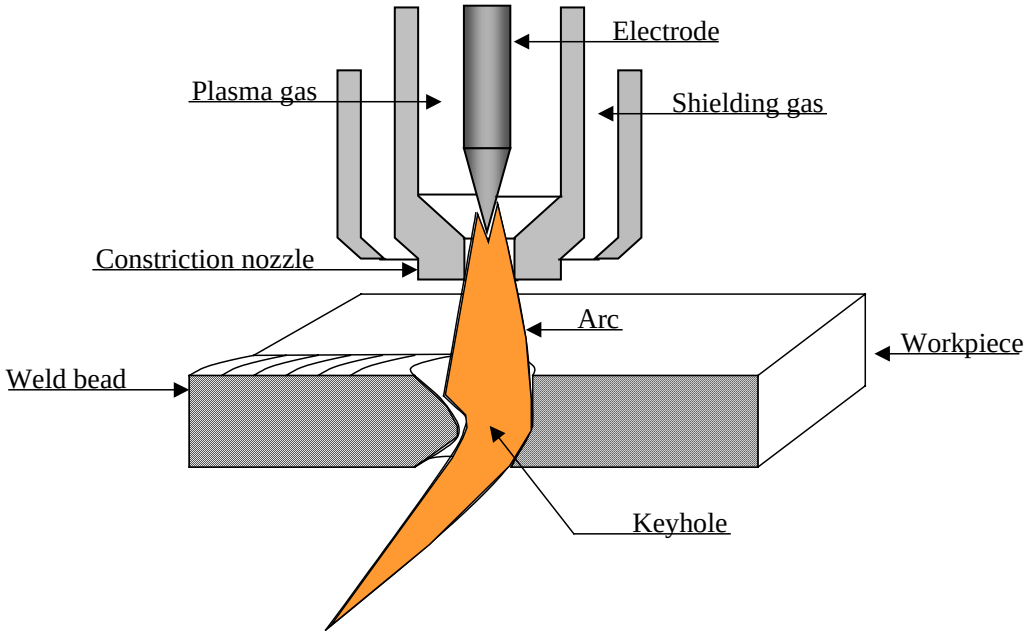

Figure 1. Keyhole plasma arc welding.

There are actually many tools applied in the modern engineering that are used to obtain mathematical models. The most common models are the statistical ones, obtained from statistical experimental designs. However, such processes are affected by a large number of variables and a generalized model will take a huge experimental design. There is also a possibility to use fractional designs, which would reduce considerably the number of experiments but would demand a great robustness of the process (Box et al., 1978). This problem may be particularly decisive when the operational ranges involved are narrow, e.g., in the case of keyhole plasma welding of carbon steel.

Another technique, the Similitude Theory, is based on dimensional analysis and is often used for machines and structures designs but not yet so used for modeling process, in particular the welding. The global idea of the similitude is that the behavior of a system or a phenomenon would be similar to a model, in scale, with the same characteristics of the original (Murphy, 1950).

In this way, the main purpose of this work is the evaluation of empirical models for keyhole plasma welding of 3,8 mm thick AISI 304L stainless steel using the Similitude Theory. These models were proposed to determine the weld bead geometry (root reinforcement and width, face width and melted zone) under certain conditions as well as to allow the process optimization considering geometry and productivity specifications. Moreover, it is intended with this work to verify the effect of the analyzed variables on the welding, allowing a general understanding of the involved phenomena in the weld formation.

2. EXPERIMENTAL PROCEDURE

It was used a digital multi-process power source with constant current electrode negative. The plasma torch used was a 300 A current capacity and its movement was controlled by a two axis XY table. The weld voltage and current signs were acquired through an acquisition data system.

Only the study variables were ranged for the system modeling. All other variables were maintained unchanged in specified values obtained from skill, manufacturer recommendations and plasma process literature. These variables and their values are listed below:

- Plasma gas: Ar;
- Shielding gas: Ar 5% O_2 (6,5 l/min);
- Purging gas: Ar (5 l/min);
- Constriction orifice diameter: 2,8 mm;
- Base metal: 3,8 mm thick AISI 304L stainless steel;
- Joint: But joint without clearance.
- Electrode: EWTh-2, ϕe 5 mm;
- Electrode vertex angle: 65°;
- Torch standoff: 5 mm;
- Electrode setback: 2,4 mm;

The electrode setback was the maximum value recommended by the plasma torch manufacturer to obtain welds in keyhole mode. The plasma gas flow rate was controlled by an equipment designed at LAPROSOLDA/UFU to measure and control the gas flow rate ranging between 0,3 and 3 l/min. The shielding and purging gases flow rates were controlled through digital gas flow meters and the cylinder pressure regulators.

It was used an image acquire and treatment software to measure the weld bead geometry. All values presented in this work are the average of 4 measures in a central part of the weld bead. The experimental design and the evaluation of the mathematical models were made using the similitude theory, presented in Murphy (1950).

3. RESULTS

3.1. Responses and dimensional analysis

The proposed responses for the weld bead geometry were root reinforcement (*RR*), root width (*RW*), face width (*FW*) and melted zone (*MZ*), as it is schematically showed in Fig. (2).

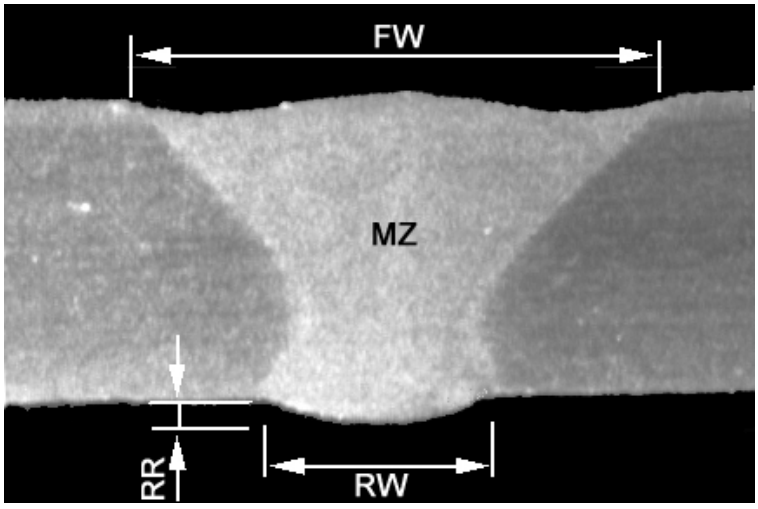

Figure 2. Characteristic weld bead profile and proposed responses.

In this away, the Eq. (1) represents the dimensional equation for *RR*, *RW* and *FW*, where ϕe is the electrode diameter, *I* is the current, *Iref* is the reference current, *Ws* is the welding speed, *PLfr* is the

plasma gas flow rate and *SHfr* is the reference flow rate. For melted zone response (*MZ*), the first term denominator must be ϕe^2 as the area unity is mm^2.

$$\frac{response}{\phi e} = f\left(\frac{I}{Iref}, \frac{Ws * \phi e^2}{SHfr}, \frac{PLfr}{SHfr}\right) \quad (1)$$

As it can be verified, all terms involved in Eq. (1) are dimensionless quantities. For each term that is varied in Eq. (1), it is obtained the isolated effect of that term on the analyzed response, which is represented by a component equation (function only of the analyzed variable). Each variable component equation may further be combined to each other by a sum function or a product function depending on their nature (Murphy, 1950). In the first case, the final response equation will be of the type *F(f(I)+f(PLfr)+f(Ws))* and, in the second case, *F(f(I)*f(PLfr)*f(Ws))*. The combination of the component equations must be validated by comparing two component equations of the same variable but obtained by varying the value of one of the dimensionless terms. In this case, the effect of plasma gas flow rate was obtained for two different values of current (170 A and 190 A). By using the theory presented in Murphy (1950), the component equations combination will be valid if similarity was found in an equality of the kind $\left[F(PLfr)_{I=190} \diagup K1\right] = \left[F(PLfr)_{I=170} \diagup K2\right]$, where K1 and K2 are constants.

The reference current (*Iref*) is a value used to make the current term into a dimensionless term. This is a random value and was chosen to be the current that the power source can supply for a 100% duty cycle. The reference flow rate (*SHfr*) used in the dimensional equation (Eq. 1) represents the shielding gas flow rate (6,5 l/min) and was introduced to obtain a dimensionless term. At the end, the *Iref* and *SHfr* are substituted by their respective values, disappearing of the final equation. The component equations of each variable on the responses proposed were selected considering their combination facility and their correlation coefficient (R^2). The minimal acceptable value for R^2 was 0,90, which ensure always good phenomenon approach. It was selected the simplest component equation to represent the effect of the variables in order to obtain single easy to work response equations.

3.2. Models evaluation

According to Richetti & Ferraresi (2001), conditions with stable keyhole are obtained when the root reinforcement is between 0,1 and 1,5 mm, which look to be the extreme limits to the keyhole conditions in this application. The initial welding condition from which the welding variables will be ranged was current 190 A, welding speed 40 cm/min and plasma gas flow rate 1,4 l/min. Such a condition provided an intermediate root reinforcement in the keyhole stability range (0,1 to 1,5 mm). This condition allows varying the dimensionless terms in both directions, to increase or to decrease the root reinforcement.

Experimental tests were carried out to obtain the isolated effect of each study variable on the responses by varying one of the dimensionless groups at a time and maintaining the others unchanged. Table (1) shows the conditions used in the experimental design and their respective results concerning the weld bead geometry.

Figures (3) to (6) show the results obtained for the effect of each study variable and the component equations for *RR*, *RW* and *FW*. Figure (3) shows the current effect on the responses (tests 1 to 6), Fig. (4) shows the welding speed effect (tests 1 and 7 to 10), Fig. (5) shows the plasma gas flow rate effect (tests 1 and 11 to 15) and Fig. (6) shows the plasma gas flow rate effect using a current level of 170 A (tests 16 to 21). In these figures, the melted zone response is not showed.

Table 1. Experimental design and results obtained for the weld bead geometry.

Test	*I* (A)	*Ws* (cm/min)	*PLfr* (l/min)	*RR* (mm)	*RW* (mm)	*FW* (mm)	*MZ* (mm^2)
1	190	40	1,4	0,46	3,22	7,07	16,22
2	160	40	1,4	0,23	2,28	6,63	13,12
3	180	40	1,4	0,34	2,95	6,99	15,03
4	200	40	1,4	0,56	3,56	7,38	17,34
5	220	40	1,4	0,78	4,34	7,63	19,14
6	240	40	1,4	1,15	5,00	7,88	21,51
7	190	30	1,4	1,15	4,92	7,63	21,03
8	190	50	1,4	0,23	2,17	6,79	13,05
9	190	60	1,4	0,13	1,64	6,42	11,99
10	190	70	1,4	0	0	6,09	9,24
11	190	40	1,0	0,24	2,18	6,83	13,40
12	190	40	1,2	0,38	3,20	7,16	15,52
13	190	40	1,6	0,59	3,97	7,30	16,99
14	190	40	1,8	0,73	4,22	7,19	17,80
15	190	40	2,0	0,93	4,34	7,18	18,32
16	170	40	1,0	0,14	1,82	6,44	12,87
17	170	40	1,2	0,25	2,63	6,56	13,97
18	170	40	1,4	0,38	3,15	6,82	15,20
19	170	40	1,6	0,45	3,39	6,75	15,63
20	170	40	1,8	0,62	3,63	6,75	16,55
21	170	40	2,0	0,73	3,91	6,90	17,30

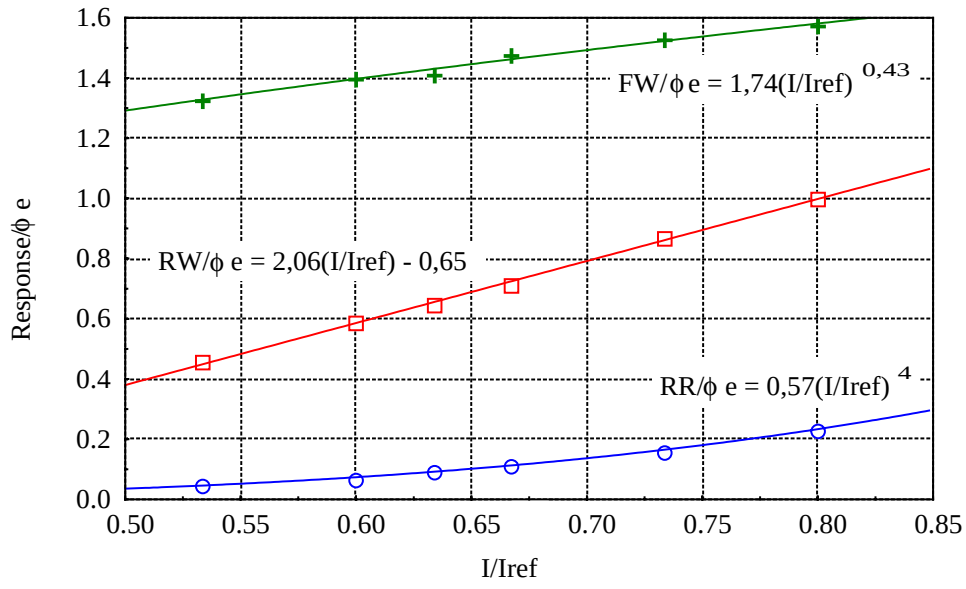

Figure 3. Current effect on the weld bead geometry.

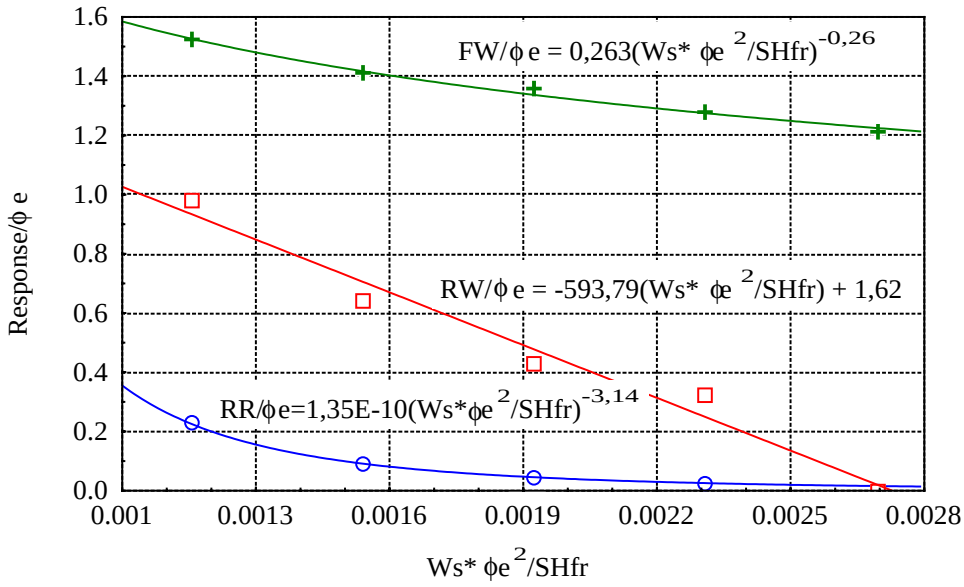

Figure 4. Welding speed on the weld bead geometry.

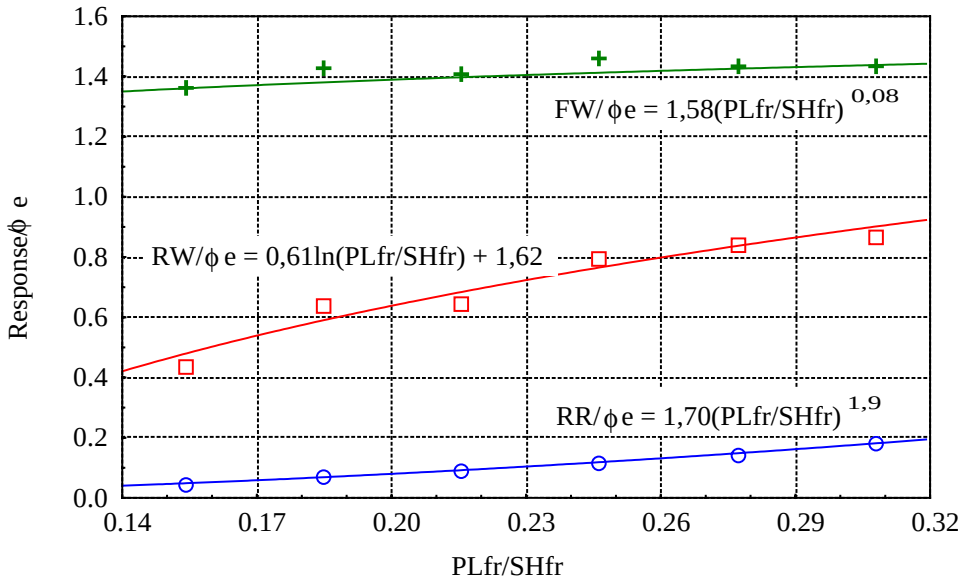

Figure 5. Plasma gas flow rate effect on the weld bead geometry.

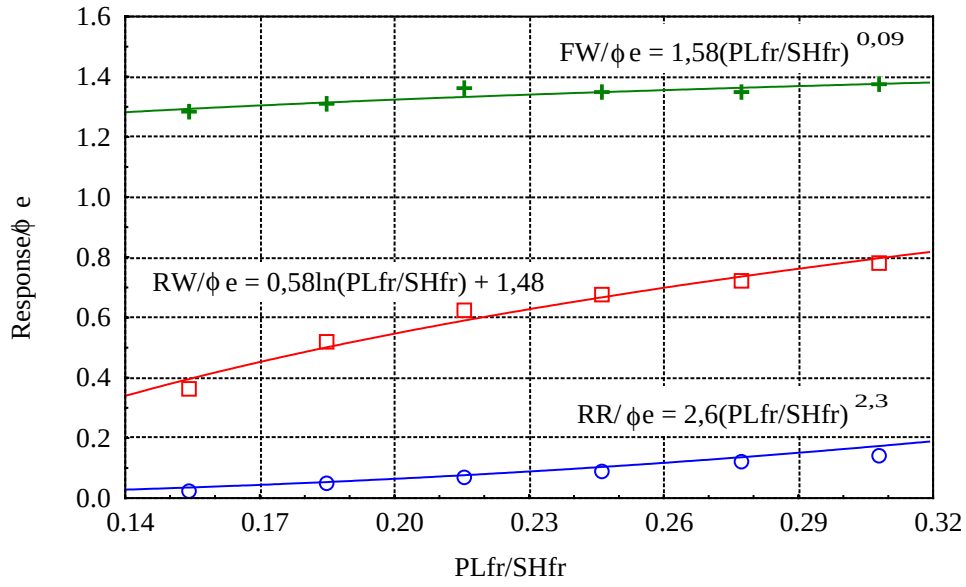

Figure 6. Plasma gas flow rate on the weld bead geometry for a current level of 170 A.

3.2.1. Weld bead root reinforcement

The component equations selected to each analyzed effect on the root reinforcement are potency functions. According Murphy (1950) their combination must be by multiplication as shown in Eq. (2).

$$\frac{RR}{\phi e} = \frac{\left[0{,}57\left(I/Iref\right)^{4}\right]\times\left[1{,}35\times10^{-10}\left(Ws\times\phi e^{2}/SHfr\right)^{-3{,}14}\right]\times\left[1{,}70\left(PLfr/SHfr\right)^{1{,}9}\right]}{(0{,}0918)^{2}} \quad (2)$$

In Equation (2), the numerator of the right side represents the multiplication of current, welding speed and plasma gas flow rate component equations. Its denominator is a constant which is the average value supplied by the components equation when the value of the initial condition (test 1: I = 190 A, Ws = 40 cm/min, $PLfr$ = 1,4 l/min, $SHfr$ = 6,5 l/min, ϕe = 5 mm and $Iref$ = 300 A) are substituted on them. This constant exponent is a number of dimensionless terms (4 with the response term) minus 2. By substituting the references values used ($Iref$ = 300 A and $SHfr$ = 6,5 l/min) it is obtained the Eq. (3) which is the general equation for the weld bead root reinforcement.

$$RR = 0{,}1\times I^{4}\times Ws^{-3{,}14}\times PLfr^{1{,}9}\times\phi e^{-5{,}3} \quad (3)$$

In this equation, the units are I [A], Ws [cm/min], $PLfr$ [l/min], ϕe [mm] and RR [mm]. According to Murphy (1950), the combination of Eq. (3) is valid if the equality presented in Eq. (4) is satisfied inside the range analyzed of $Plfr/SHfr$ (0,15 a 0,31), showing similarity of the plasma gas flow rate effect for both current levels 190 A and 170 A.

$$\frac{1{,}70\left(PLfr/SHfr\right)^{1{,}9}}{0{,}092} = \frac{2{,}60\left(PLfr/SHfr\right)^{2{,}3}}{0{,}076} \quad (4)$$

The numerators in Eq. (4) are the component equations of plasma gas flow rate for both current levels 190 A e 170 A, showed in Figs. (5) and (6), respectively. The denominators are values supplied by these equations when the initial condition value of *PLfr/SHfr*, i.e. 1,4/6,5, is substituted on them. By varying the *PLfr/SHfr* value inside the work range (0,15 to 0,31) in Eq. (4), it was verified that the encountered deviations comparing both side of the equation were low, at least 16%, validating the combination made in Eq. (3).

3.2.2. Weld bead root width

The components equations selected for the effects on the root width are lines (y = ax + b) and they suggest a combination by sum. This combination is showed in Eq. (5).

$$\frac{RW}{\phi e} = \left[2{,}06\left(\frac{I}{Iref}\right) - 0{,}65\right] + \left[-593{,}79\left(\frac{Ws * \phi e^{2}}{SHfr}\right) + 1{,}62\right] + \left[0{,}61 \times \ln\left(\frac{PLfr}{Shfr}\right) + 1{,}62\right] - 2(0{,}681) \quad (5)$$

The Equation (5) is a sum of the component equations for the root width. The last term in this equation is a constant, obtained by the average of the values supplied by each component equation when the values of the initial condition (test 1) are substituted on them. The number multiplied to this constant is the number of dimensionless groups (4 with the response term) minus 2. Substituting the references values used into Eq. (5) it is obtained the Eq. (6), which is the general equation for the root width.

$$RW = [6{,}87 \times 10^{-3}(I) + 0{,}61\ln(PLfr) - 9{,}14 \times 10^{-4}(Ws)(\phi e)^{2} + 0{,}09] \times \phi e \quad (6)$$

The combination validity test is done through the Eq. (7). In this equation the terms between square bracket are the plasma gas flow rate component equations for both current levels 190 A and 170 A, showed in Figs. (5) and (6) respectively. The terms that are subtracted in both side of this equation are the values obtained from the respectively component equation when the initial condition *PLfr/SHfr* = 1,4/6,5 is substituted on them. Then substituting the values of *PLfr/SHfr* inside the work range (0,15 to 0,31) it is obtained a maximum similarity deviation of approximately 6% validating the combination made in Eq. (6).

$$\left[0{,}61\ln\left(PLfr \middle/ SHfr\right) + 1{,}62\right] - 0{,}683 = \left[0{,}58\ln\left(PLfr \middle/ SHfr\right) + 1{,}48\right] - 0{,}590 \quad (7)$$

3.2.3. Weld bead face width and melted zone

By applying the same procedure presented above it is obtained the Eqs. (8) and (9) for face width and melted zone respectively. In both cases, the similarity deviations encountered in the validity test were lower than 1%, validating the combination evaluated. The component equations for the melted zone response were not showed in this work.

$$FW = 0{,}87 \times I^{0{,}43} \times Ws^{-0{,}26} \times PLfr^{0{,}08} \times \phi e^{0{,}48} \quad (8)$$

$$MZ = 0{,}56 \times I^{1{,}21} \times Ws^{-0{,}92} \times PLfr^{0{,}43} \times \phi e^{0{,}16} \quad (9)$$

4. MODEL EXPERIMENTAL VALIDATION

The models consistency were experimentally tested by comparing the weld geometry measured and predicted in 3 different welding conditions. The others process variables were maintained constants in the values presented in the items 2 and 3.2 of this work. Table (2) shows the results obtained in these tests. It can be seen that the predicted values are very close to the measured ones. It suggests that the models obtained may be safely used to predict the weld bead geometry in this application.

Table 2. Results obtained in the model experimental validation tests.

Variable	Condition 1		Condition 2		Condition 3	
Current (A)	170		210		230	
Welding speed (cm/min)	45		55		65	
Plasma gas flow rate (l/min)	1,45		1,75		1,90	
Measure	Measured	Predicted	Measured	Predicted	Measured	Predicted
RR (mm)	0,19	0,22	0,37	0,38	0,34	0,38
RW (mm)	2,13	2,18	2,90	2,96	2,66	2,74
FW (mm)	6,37	6,59	6,94	6,95	7,17	6,97
MZ (mm^2)	12,50	12,72	14,71	14,81	14,75	14,69

5. RESULTS INTERPRETATION

The models obtained for *RR*, *RW*, *FW* and *MZ* responses are valid in the range of the variables analyzed and in the same conditions used. By substituting the values of current (A), welding speed (cm/min) and plasma gas flow rate (l/min) into the models it is possible to predict the weld bead geometry. However, it is important to take into account how to interpret the results with such models.

The main indication of the keyhole formation is the resultant weld root. However, the result interpretation may be important to detect extreme conditions like as excessive or incomplete penetration. Incomplete penetration may be predicted in this application when the predicted root reinforcement is up to approximately 0,1 mm. On the other hand, when the root reinforcement and root width are too high it means a condition of excessive penetration. This assessment is made by the welder skill but in this application and for the conditions studied it may be predicted when the root reinforcement is at about 1,5 mm or greater or the root width is greater than 5 mm. These are the physical limits for the weld pool maintenance.

6. PROCESS OPTIMIZATION

An optimized welding condition evaluated from the models was tested through a sequential optimization software (DOT – *Design Optimization Tools*, version 4.20). The optimization methods used were Modified Method of Feasible Directions (MMFD) and Sequential Quadratic Programming (SQP) (Vanderplaats, 1984). The optimized condition was obtained by the maximization of an objective function presented in Eq. (10) considering the models evaluated and the imposed constraints.

$$Objective\_Function = Ws / I \tag{10}$$

The objective function was defined using productivity and nozzle wear criteria. How can be seen in Eq. (10), it is wished a maximum welding speed and a minimum current to maximize the objective function. The welding speed is related to productivity and the current level to the temperatures in the

nozzle. The boundary conditions were the weld bead geometry that was specified according to practical skill. For each optimization method MMFD and SQP it was used 6 initial estimates from which the software tried to maximize the objective function into the experimental work range. Only the best result of each optimization method was selected. The weld bead geometrical specification (boundary conditions) were **RR= 0,4 mm; RW= 3,0 mm; FW= 7,0 mm**.

Table (3) shows the optimized conditions for each method used and the results obtained in experimental tests. In this table, it is verified that the experimental results are very close to the predicted ones. The results suggest that the models evaluated are consistent and can be used to determine the final weld bead geometry into the work range and to optimize the welding condition.

Table 3. Predicted and experimental results using the optimized condition.

Initial estimate (*I* = 220 A, *Ws* = 70 cm/min e *PLfr* = 1,8 l/min)	Optimization method		Experimental tests		
	MMFD	SQP	Test 1	Test 2	Test 3
I (A)	219	219	219	219	219
Ws (cm/min)	57,5	57,5	57,5	57,5	57,5
PLfr (l/min)	1,76	1,76	1,76	1,76	1,76
RR (mm)	0,4	0,4	0,43	0,41	0,46
RW (mm)	3,0	3,0	3,16	2,89	3,08
FW (mm)	7,0	7,0	6,99	6,94	6,94
MZ (mm^2)	15,0	15,0	15,82	14,47	14,87
Objective function - Eq. (10)	0,262	0,263	-	-	-

7. CONCLUSIONS

- The methodology used allows to obtain consistent models to predict the weld bead geometry.
- The current affected proportionally the weld bead dimensions analyzed (*RR*, *RW*, *FW* and *MZ*).
- The welding speed was inversely proportional on the weld bead dimensions *RR*, *RW*, *FW* and *MZ*.
- The plasma gas flow rate was proportional in all dimensions analyzed (*RR*, *RW*, *FW* and *MZ*).
- The condition optimization through the maximization of a objective function was possible and the predicted dimensions were very close to the measured ones.

8. ACKNOWLEDGEMENTS

The authors would like to thank ACESITA S.A. for material donation and CAPES for financial support.

9. REFERENCES

Box, G. E. P., Hunter, W. G. & Hunter, J. S., 1978, “Statistic for Experimenters - An Introduction to Design, Data Analysis, and Model Building”, John Wiley & Sons, Inc., p. 652.

Murphy, G., 1950, “Similitude in Engineering”, The Ronald Press Company, 199 p.

Richetti, A. & Ferraresi, V. A., 2001, “Prediction of weld bead geometry and optimization of keyhole plasma welding of AISI 304L stainless steel”, 16th Brazilian Congress of Mechanical Engineering, November 26 - 30, Uberlândia, MG, Brazil, CD-ROM.

Vanderplaats, G. N., 1984, “Numerical Optimization Techniques for Engineering Design with Applications”, McGraw Hill, 333p.